

New technique for dynamic-range compression and contrast enhancement in infrared imaging systems

Zhao Yaohong^{1,2,3}, Wang Yuanyuan^{1,2,3,4}, Luo Haibo^{1,2,3}, Li Fangzhou^{1,2,3,4}

(1. Shenyang Institute of Automation, Chinese Academy of Sciences, Shenyang 110016, China;

2. Key Laboratory of Opto-Electronic Information Processing, Chinese Academy of Sciences, Shenyang 110016, China;

3. The Key Lab of Image Understanding and Computer Vision, Liaoning Province, Shenyang 110016, China;

4. University of Chinese Academy of Sciences, Beijing 100049, China)

Abstract: Dynamic range compression and detail enhancement are two important issues for effectively displaying high dynamic range infrared (IR) images on standard dynamic range monitors. Sophisticated techniques are required in order to improve the visibility of the details without introducing distortions. A novel method was introduced for visualization of IR images. The proposed method was composed of two cascaded steps. In the first step, dynamic range compression of infrared images was posed as an quadratic optimization problem that minimize a cost function. In the second step, the detail was enhanced by an specifically designed exponential factor that provided excellent detail visibility and avoid halo artifacts. The performance of the proposed technique was evaluated using a data set of IR images collected from different operating conditions. The results show that the proposed method is insensitive to features occurring in IR image and yield the most visually pleasing outputs. Compared with other algorithms, it can effectively improve the overall contrast, prevent over-enhancement of flat regions and reduce noise visibility.

Key words: dynamic range compression; detail enhancement; infrared images; high dynamic range

CLC number: TN219 **Document code:** A **DOI:** 10.3788/IRLA201847.S126001

红外成像系统中的高动态范围压缩与对比度增强新技术

赵耀宏^{1,2,3}, 王园园^{1,2,3,4}, 罗海波^{1,2,3}, 李方舟^{1,2,3,4}

(1. 中国科学院沈阳自动化研究所, 辽宁 沈阳 110016;

2. 中国科学院光电信息处理重点实验室, 辽宁 沈阳 110016;

3. 辽宁省图像理解与视觉计算重点实验室, 辽宁 沈阳 110016; 4. 中国科学院大学, 北京 100049)

摘要: 动态范围压缩和对比度增强是红外成像的两个关键步骤, 如何提升图像细节、抑制失真是红外成像的重要研究课题。提出了一种新的红外图像可视化方法。算法首先通过最小化损失函数的方法将动态范围压缩问题转化为一个二次优化问题; 然后通过设定一个指数因子来增强细节, 最终能够在提升细节的同时避免产生光晕。使用不同场景采集的多组红外图像进行实验, 结果表明所提算法不仅

收稿日期: 2018-03-17; 修订日期: 2018-04-30

基金项目: 中国科学院国防创新基金(CXJJ-15-S109)

作者简介: 赵耀宏(1979-), 男, 研究员, 硕士生导师, 博士, 主要从事图像处理等方面的研究。Email: zhaoyaohong@sia.cn

对红外图像的固有特征有很好的抗性,而且处理结果较好。对比其他算法,该方法能够有效提高图像整体对比度,防止平坦区域过度增强,并且抑制了噪声。

关键词: 动态范围压缩; 细节增强; 红外图像; 高动态范围

0 Introduction

Modern thermal cameras have increased sensitivity and typical noise equivalent temperature difference (NETD) can reach 10 mK. This means that temperature changes of 50 K within the monitored scene will produce a dynamic range around 5 000, which roughly corresponds to 12–13 bits. This high dynamic range (HDR) image cannot be easily managed by state-of-the-art displays, which can only show 256 gray levels, corresponding to 8 bits. Therefore, a procedure is required to adapt data from the detector to the display. This procedure must accomplish three goals: (1) Compressing the dynamic range of the input image into a low range one that is acceptable for the display system. (2) Enhancing the contrast according to IR features occurring in images without excessively distorting the radiometric IR information. (3) The output image is pleasing to the human observer.

The problem for the visualization of HDR images has been widely investigated and a number of techniques has been proposed. For HDR infrared images visualization, the techniques can be divided into two broad groups: global approaches and local approaches.

Automatic gain control (AGC)^[1] and Histogram equalization(HE)^[2] are two widely used global methods. Plateau HE(PE)^[3-4] has been proposed to display infrared images by reducing the enhancement of homogeneous regions with a plateau threshold value. A general framework based on histogram equalization for image contrast enhancement is presented^[5], which employs carefully designed penalty to adjust the various aspects of contrast enhancement. In summary, global approaches lack flexibility in manipulating small

details of the raw input images, because they do not use the neighboring information.

Local approaches use local information to build the transformation functions. Thus, these methods have more power to enhance the local contrast compared to global approaches. The balanced CLAHE and contrast enhancement(BCCE)^[6] techniques exploit local contrast enhancement to improve the visualization of low-contrast details and manage the output dynamic in the presence of large intensity variations. In the framework of unsharp masking(UM) approaches^[7-12], there are two main drawbacks which is noise amplification in uniform areas and generation of artifacts due to over enhancement of high-frequency details^[7-8]. In the literature, several techniques have been proposed to improve UM performance. In the BF&DRP method^[9-10], bilateral filtering is adopted to separate the detail layer from the base component, and then the two components are handled, respectively. Zuo^[11] et al. proposed an improved version of BF&DRP, here we call it BF&DDE. This approach relies on adaptive Gaussian filtering to avoid over enhancing artifacts. However, halos are unavoidable for local filters when the filters are forced to smooth some edges^[13]. Liu^[12] et al. presented an improved version of BF&DDE. This approach is based on the guided image filter and separates the acquired image into the base layer and the detail layer, and then processed each part independently. Since the guided image filter is a locally based operator, it may have halos near some edges.

Among these techniques, it is worth noting that issues such as noise increase and IR features preservation have not been properly managed. In this work, we proposed a new method for visualization of IR images aiming at meeting the challenging requirements must be satisfied by operating IR

sensors. The proposed method named as histogram modification based dynamic range compression and contrast adjustment (HMCA). The proposed method is a two-step method: (1) A DRC step by means of histogram modification. (2) A local contrast enhancement step using an exponential factor. The proposed HMCA approach has been experimentally evaluated using a set of IR images data collected with a modern IR device on different operating situations of surveillance scenarios. The performance of the proposed technique has been compared with that of previously proposed techniques in the literature of IR image processing. HMCA can assure good performance in different operating conditions.

1 Proposed algorithm

Here, we propose the HMCA algorithm. Figure 1 shows the block scheme of the proposed technique. The proposed method consists of two separate and cascaded processing blocks: DRC and local contrast enhancement. The DRC is used to effectively exploit the entire output dynamic range, while local contrast enhancement is used to improve the visualization of low contrast details. In the DRC block, we first gather the histogram information from the input image. Then a quadratic optimization framework is used to obtain the modified histogram \hat{h} . Subsequently, we reduce

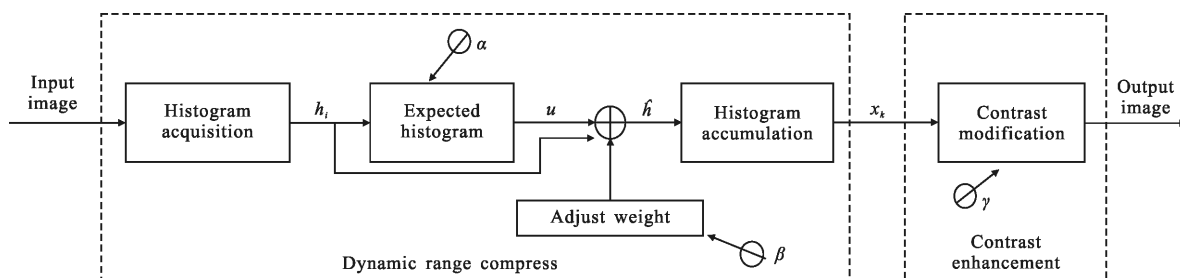


Fig.1 Block diagram of the proposed HMCA algorithm

the dynamic range of input image using the modified histogram \hat{h} . In the second block, we enhance the local contrast using an exponential factor provides an excellent visibility of details avoiding halo artifacts. Three parameters α , β and γ regulate the performance of the method.

1.1 Dynamic range compression based on histogram modification

Arici^[5] et al. proposed a histogram modification framework for visible spectral image contrast enhancement. In this framework, histogram modification is posed as an optimization problem to minimize a cost function. This study showed that the contrast of visible spectral image can be improved without introducing visual artifacts. In this work, we adopted the framework to perform DRC of IR image. Let column vector h_i denote the histogram of input image and column vector u is specified the desired

histogram. The modified histogram is generated by minimizing the following cost function:

$$\min \|h-h_i\| + \lambda \|h-u\| \quad (1)$$

where h , h_i and $u \in R^{L-1}$, L represents the range of input pixel value; λ is regularization parameter. This is a bi-criteria optimization problem and when the Euclidean norm is used, Eq.(1) becomes

$$\hat{h} = \underset{h}{\operatorname{argmin}} \|h-h_i\|_2^2 + \lambda \|h-u\|_2^2 \quad (2)$$

where $\hat{h} \in R^{L-1}$ is the optimized histogram in this problem which results in the quadratic optimization problem

$$\hat{h} = \underset{h}{\operatorname{argmin}} [(h-h_i)^T(h-h_i) + \lambda(h-u)^T(h-u)] \quad (3)$$

Analytical solution of Eq.(3) is

$$\hat{h} = h_i / (1+\lambda) + \lambda u / (1+\lambda) \quad (4)$$

If we define κ as

$$\kappa = 1 / (1+\lambda) \quad (5)$$

The \hat{h} can be expressed as

$$\hat{h} = \kappa h_i + (1 - \kappa)u \quad (6)$$

So the modified histogram \hat{h} is a weighted average of the input histogram h_i and the desired histogram u .

After histogram modification, \hat{h} can be accumulated to map input pixels to output pixels similar to HE. Let $T(n)$ denote the transform function, which maps intensity n in the input image to intensity $T(n)$ in the output image. The transform function $T(n)$ is obtained by

$$T(n) = \lfloor \frac{(D-1)}{MN} \sum_{j=0}^n \hat{h}(k) + 0.5 \rfloor \quad (7)$$

where $\hat{h}(k)$ denotes the number of pixels, which is resident within the histogram bin of for gray level k ; D denotes the maximum intensity of the output image. Noting that $D=256$ when an 8-bit image is considered. M, N is the row and column of the input image, respectively, and $\lfloor a \rfloor$ is the floor operator and returns the largest integer smaller than or equal to a .

1.1.1.1 Desired histogram

According to Eq. (6), the output image depends on desired histogram u , so the choice of suitable u is a critical part of the proposed algorithm. In general, the desired histogram u should choose a uniformly distributed vector as stated in Ref [5], because a uniformly distributed output histogram fully exploits the available dynamic range. However a suitable choice of desired histogram u should take account of some of the characteristics of IR images^[6]. First, it is desirable to exploit the full dynamic range of the output gray levels for HDR input taking account of some of the characteristics of IR images. Second, dramatically change the global intensity of the display is unacceptable when very hot or very cold small target comes into the field view.

Taking into account the aforementioned conditions, we proposed an approach to set the desired histogram u . The motivation is to set u according to

h_i , that is

$$u = P(h_i) \quad (8)$$

where the function P is used to map the h_i to u .

The histograms of the HDR infrared images usually contain many unoccupied gray levels. For example, the horizon effect may create a situation in which the input histogram is nearly zero between the two lobes associated with ground and sky. If we chose a uniformly distributed vector, the output dynamic range will not be completely filled, which disregards the already limited output display levels. Thus, by considering this characteristic of the infrared images, we adopted histogram projection to determine P .

In the histogram projection method, we first obtain an binary histogram $b(k)$ like histogram projection method. If one specific gray level is occupied by one or more pixels, this level is considered valid and the output range is assigned equally to each valid gray level present. The histogram projection could effectively reproduce the shape of the raw signal histogram aside from the omission of the unoccupied levels. However, under conditions of scenes with wide dynamic ranges, it tends to produce too little contrast where it is needed since the output range is filled by gray levels occupied by a very small number of pixels. So a improved version of histogram projection is adopted^[11]. The original histogram of is binarized using a threshold α :

$$b(k) = \begin{cases} 1 & h_i(k) \geq \alpha \\ 0 & h_i(k) < \alpha \end{cases} \quad (9)$$

where $h_i(k)$ denotes the number of pixels that is resident within gray level k . The purpose of threshold α is to reduce the influence of small hot or cold object, which dramatically changes the global intensity of the display. When $h_i(k)$ is larger than the threshold α , it means that the gray level k can be found frequently in the original image and should be preserved in the output.

Finally, according to $b(k)$, the desired histogram is assigned equally to each valid bin regardless of how many pixels occupy that level, that is

$$u(k) = \frac{MN}{\sum_{k=0}^{L-1} b(k)} b(k) \quad (10)$$

1.1.2 Choices of adaptive regularization parameter κ

For bi-criteria optimization problem in Eq. (6), the regularization parameter κ plays an important role. By adjusting κ , a compromise is achieved to improve the perceptibility of the details and suppress contrast over-stretching. From Eq. (6), if κ is too large, the modified histogram \hat{h} is close to the input histogram h_i . Therefore standard HE is applied in Eq.(7), which may cause contrast over-stretching. If κ is too small, the penalty term comes into play and the enhanced image looks more like histogram projection, which may produce too little contrast. In Ref. [5], κ is computed by measuring the input contrast using the aggregated outputs of horizontal two-lagged difference operation. Afterwards, κ is multiplied by a user-controlled parameter. It is time consuming and the user-controlled parameter may need tune by hand for different images.

In this work, we proposed a new method to adaptively set the κ according to the input image. Let $T(n, \kappa)$ denote the transform function of Eq.(7) for a given regularization parameter κ . We chose κ in such a way that the maximum backward-difference of $T(n, \kappa)$ is limited by parameter β , that is

$$\max[\Delta T(n, \kappa)] = \beta \quad (11)$$

where $\Delta T(n, \kappa)$ denotes the backward-difference of $T(n, \kappa)$. In general, the parameter β is less than 1. This constraint makes sure that contrast of output image will not be over-stretching. The suitable κ can be obtained by solve this equation. If we ignore the rounding-off operation in Eq. (7), we can get a recurrence equation:

$$\Delta T(n, \kappa) = T(n, \kappa) - T(n-1, \kappa) = \hat{h}(k)(D-1)/MN \quad 1 \leq k \leq L-1 \quad (12)$$

From Eq.(12), it is easy to see that transform function has sharp transition when the value of $\hat{h}(k)$ is large. For IR image, the histogram occupancies at the peak of the histogram is relatively high, so the

maximum back-ward-difference of $T(n, \kappa)$ always occurs at the peak of the histogram, that is

$$\max[\Delta T(n, \kappa)] = \hat{h}^p(D-1)/MN \quad (13)$$

where \hat{h}^p denotes the histogram peak value of \hat{h} . From Eq.(6), \hat{h}^p is given by

$$\hat{h}^p = \kappa h_i^p + (1-\kappa)u^p \quad (14)$$

where h_i^p is the histogram peak value of and u^p is the histogram peak value of u . From Eqs.(13) and (14), we can get the following equation

$$[\kappa h_i^p + (1-\kappa)u^p](D-1)/MN = \beta \quad (15)$$

The desired κ can be obtained by solving Eq.(15), that is

$$\kappa = \frac{\beta MN - u^p(D-1)}{(h_i^p - u^p)(D-1)} \quad (16)$$

A simple analysis can help us to understand this seemingly complicated equation. From Eq.(16), for a given β and u^p , κ is roughly in inverse proportion to h_i^p . For low contrast input images, the histogram of input image has a concentrated distribution corresponding a large h_i^p . So we chose small κ and \hat{h} is close to u . In this manner, the output of Eq. (7) is more like histogram projection, which avoid contrast over-stretching. On the contrary, for high contrast images, the histogram of input image has flat distribution corresponding a small h_i^p . So we chose large κ and the output of Eq.(7) is more like HE, which produces good contrast. In such a way, the regularization parameter κ is set adaptively according to the content of input image.

1.2 Contrast enhancement

It should be pointed out that the global histogrambased methods could compress the dynamic range of the raw images effectively, but they lack flexibility in manipulating small details of the raw input images, since they are based only on histogram information. So a further adjustment of the local contrast is necessary for the purpose of improving the visibility of details in poorly contrasted areas. In this

context, we adopted local image contrast preservation theory as in Ref. [14] to adjust contrast by a new weighting function. The local image contrast preservation theory adjusts contrast according to local contrast image $C(i,j)$, which is defined as

$$C(i,j)=f_{\text{drc}}(i,j)/f_{\text{drc}}^M(i,j) \quad (17)$$

where $f_{\text{drc}}(i,j)$ and $f_{\text{drc}}^M(i,j)$ are the image after DRC and the related lowpass version of $f_{\text{drc}}(i,j)$. The output image after contrast enhancement $f_{\text{drcca}}(i,j)$ is obtained by multiplying the image $f_{\text{drc}}(i,j)$ with a weighting function $w[C(i,j)]$, that is

$$f(i,j)_{\text{drcca}}=f_{\text{drc}}(i,j)w[C(i,j)] \quad (18)$$

The local image contrast preservation theory is based on the observation that $C(i,j)$ is an edge indicator function. We show a typical IR image after DRC in Fig.2(a). In Fig.2(b), we report the corresponding $C(i,j)$ of Fig.2(a), which is computed by a Gaussian lowpass filter with a 5×5 window and standard deviation of two pixels. It is easy to verify that, for flat area, $C(i,j)$ is near 1. On the contrary, For strong edge of building the corresponding of $C(i,j)$ is close to 0 or 2. Furthermore, the histogram of $C(i,j)$ is reported in Fig.2(c), it can be seen that $C(i,j)$ are distributed over 0 to 2.

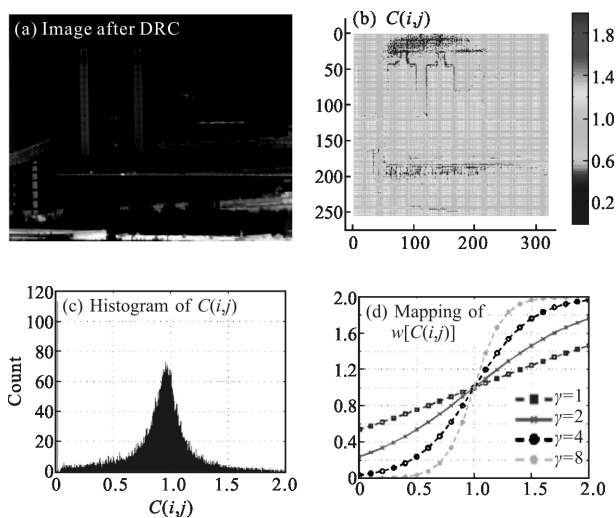


Fig.2 Contrast enhancement

From Eq.(18) the weighting function $w[C(i,j)]$ plays an key role in the contrast enhancement. A

suitable weighting function should meet the following requirements^[14]. In general, pixels in flat area, which are characterized by unitary contrast [$C(i,j)=1$] should left unchanged to prevent enhancement of noise visibility. Pixels in low contrast areas, which are characterized by near 1 contrast [$C(i,j) \approx 1$] should have big gains to ensure better enhancement. Pixels in high contrast areas, which are characterized by large contrast like strong edge of building should set a limited expansion of the contrast to avoid halo artifacts. To satisfy aforementioned condition, an specifically weighting function $w[C(i,j)]$ is designed, that is

$$w[C(i,j)]=\frac{2}{1+\exp[\gamma(1-C(i,j))]} \quad (19)$$

where γ is the parameter regulates shape of $w[C(i,j)]$. It should point out that $w[C(i,j)]$ satisfies the requirement of different class of input image. Figure 2(d) shows the plot of $w[C(i,j)]$ with four different γ . It is easy to verify that for pixels in flat area ($C(i,j)=1$), the corresponding $w[C(i,j)]=1$. So the pixel's contrast left unchanged. For pixels in low contrast areas, the contrast has been expanded according to γ . Meanwhile, it is easy to see that big values of γ causes a steep slop of $w[C(i,j)]$, while small values of γ causes a flat slop of $w[C(i,j)]$. So the parameter γ determines the degree of the needed contrast. The setting of the parameter γ will be discussed in the following section.

2 Experimental results and discussion

To test the proposed technique in different operating conditions, we collected IR image with a 320×256 HgCdTe IRFPA with 14-bit output raw data. Then we processed the captured raw image data and chose three samples as test image. The test images have been selected with different characteristics, such as small hot objects, horizon line, flat areas. The images shown in Fig.3–5 have been visualized using AGC with saturation of 0.1% of outliers at both bottom and top ranges of the dynamic. IM#1 shows a typical image with long tailed-histogram images. IM#2 shows a complex surveillance scenes with a higher

percentage of valid gray levels. IM#3 represents a maritime scenario and two objects located at a medium range in the field of view. A brief description of the test sequences is summarized in Tab.1. Each image is denoted by a IM# plus number. We report the dynamic range in digital levels (DL) and the percentage of the actual DL.

Tab.1 Description of the test image sequences

Image	Max(DL)	Min(DL)	DL	Percentage of DL
IM#1	15 512	13 346	1 738	11%
IM#2	18 977	12 843	2 026	12%
IM#3	1 633	2 851	10 910	67%

2.1 Choices of the parameter

Relating to the block scheme in Fig.1, the proposed technique for the visualization of IR HDR images depends on the three parameters α , β and γ .

2.1.1 Choice of the parameter α

The purpose of threshold α is to reduce the influence of small hot or cold object, which dramatically changes the global intensity of the display. When $h_i(k)$ is larger than the threshold α , it means the gray level k can be found frequently in the original image and should be preserved in the output. It is reasonable to choose threshold α according to the sizes of outliers. In the experiments, we set outliers pixel size as 10×10 , which is 0.1% of the total number of pixels for 320×256 image.

2.1.2 Choice of the parameter β

The parameter β is defined as allowable backward-difference value of $\Delta T(n, \kappa)$. For a given β , the problem parameter κ is adaptively set according to h_p . The advantage of β is that for most images it could have the same value. For a given image, the problem parameter κ is proportional to β . Big values of β causes the modified histogram \hat{h} close to the input histogram h_i , while small values of β causes the modified histogram more like u . We tried the set of β values 1/4, 1/2 and 1 on a number of images and

found that β of 1 appeared to be a generally upper-limit. Meanwhile, β of 1/2 always gives a pleasing result.

2.1.3 Choice of the parameter γ

The effectiveness of contrast adjustment strictly depends on the setting of the parameter γ . In fact, the rate slop of $w[C(i;j)]$ determines the contrast. According to Eq.(19), the rate slop is given as

$$\frac{\partial w}{\partial C} = \frac{2\gamma e^{\gamma(1-C)}}{[1+e^{\gamma(1-C)}]^2} \tag{20}$$

The rate of slop at $C=1$ is $\gamma/2$. In general, values of $\gamma > 2$ can enhance local contrast. On the contrary, values of $\gamma < 2$ can smooth the output image. It can be noted that the γ of 4 gives a satisfactory result. In the experiments, we have noticed that a value of 4 always yields satisfactory results.

2.2 Compared algorithms

The proposed method was compared with five visualization techniques, i.e., AGC [1], HE [2], PE [3-4], BF&DRP [9] and BF&DDE [11]. In our experiments, the parameters values of other five methods are set according to the original papers.

2.2.1 Quantitative tests

In the quantitative comparison, the metric used to quantitatively evaluate the enhancement effect of different methods is given by the root-mean-square contrast (RMSC) and measure of enhancement (EME). RMSC is defined as [15]

$$RMSC = \sqrt{\frac{1}{MN} \sum_{ij} (I(i,j) - \bar{I})^2} \tag{21}$$

where \bar{I} is the average intensity of all pixel values in the image; M and N are image's row and columns, respectively. EME is defined as [16]

$$EME = \frac{1}{k_1 k_2} \sum_{i=1}^{k_1} \sum_{j=1}^{k_2} 20 \ln \frac{\max(X_{i,j})}{\min(X_{i,j})} \tag{22}$$

where the input image be divided into nonoverlapping sub-blocks $X_{i,j}$; $\max(X_{i,j})$ and $\min(X_{i,j})$ are the maximum and minimum gray levels, respectively in block $X_{i,j}$.

The contrast results are given in Tab.2. It can be seen that HE, PE and the proposed method have

higher RMSC in the mean scene, while BF&DDE and HMCA have higher EME. It should point out that the contrast metric can help but it does not necessarily indicate good visual effects. Therefore, a subjective evaluation is necessary.

Tab.2 Mean RMSC and EME results for the three test images

Image	AGC	HE	PE	BF&DRC	BF&DDE	HMCA
RMSC IM#1	39.76	73.43	56.21	38.63	44.01	49.69
RMSC IM#2	32.00	73.57	62.07	31.60	42.67	59.45
RMSC IM#3	55.17	73.77	75.30	55.30	55.41	67.16
EME IM#1	2.97	11.12	10.89	13.76	23.66	23.28
EME IM#2	3.69	6.09	6.21	8.05	11.17	12.96
EME IM#3	2.10	4.58	4.56	4.37	9.72	9.13

2.2.2 Subjective tests

We present the image processed by the compared algorithms and our algorithms in Fig.3–5. The results show that AGC maps the original dynamic range to the display range linearly without doing any enhancement of contrast adjustment. Because the AGC mapping is a global tone mapping operator that does not consider the intensity differences of the neighboring pixels to reproduce the local details. Histogram equalization can change the overall contrast to a certain degree, but it tends to over-enhance the background. For example, in Fig.3 (b) and Fig.4(b) the building is over-enhanced and produces some annoying artifacts. PE has been proven to be more effective and can achieve adequate compression of the dynamic range, but it often shows poorly contrasted image. The structures of the coast in Fig.5 (c) is obscured. The overall contrast of BF&DRP result is a resemblance to that of the AGC, while the details show a great improvement. But it sometimes produces severe gradient reversal artifacts and highlights the noise in flat regions. BF&DDE is clearly superior in detail protection compared to BF&DRP, but it cannot get rid of gradient flipping artifacts completely. In

addition, it is very sensitive to noise. Such as the one shown in Fig.5(e), the result has unpleasant artifacts.

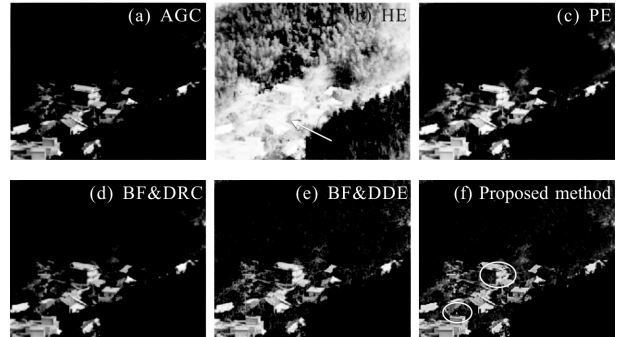


Fig.3 IM#1 comparison results

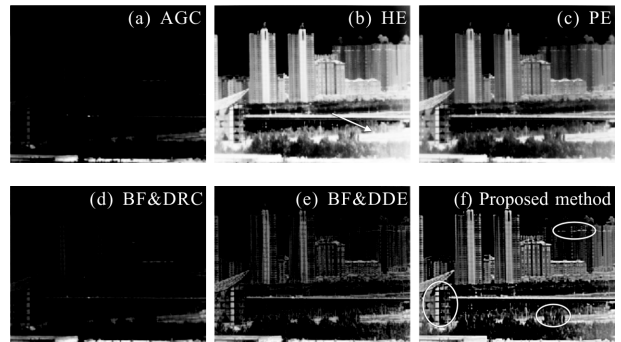


Fig.4 IM#2 comparison results

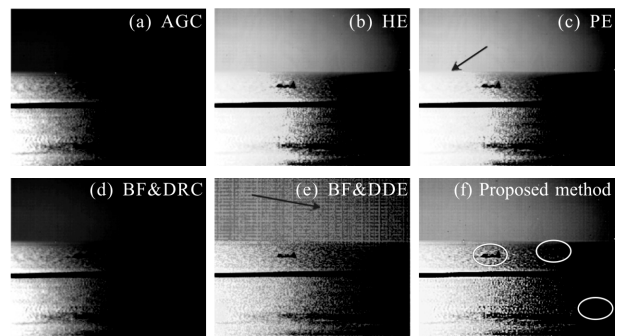


Fig.5 IM#3 comparison results

Focusing on the HMCA technique, it effectively reduces the dynamic range of the input image without excessively distorting the radiometric IR information and has the good results concerning details visibility compared to the other methods. As shown in Fig.3, the proposed method yields the most visually pleasing outputs, the entire image looks natural and clear. It is free of halo, gradient reversal and saturation artifacts. As shown in Fig.4(f), it has the better visibility of buildings than other methods. Furthermore, HMCA

prevents over enhancement of flat regions and reducing noise visibility. We would like to point out that the HMCA method has been designed to display images with constraints of reducing noise visibility. As shown in Fig.5, all targets are detected by HMCA and the sky region in are well managed without overenhancement. This is because the values of gains of the sky region are near 1, which prevents amplification of noise in that region. Finally, the HMCA is robust and insensitive to features occurring in IR image such as hot objects and horizon effect. We found in our experiments that for the specific scenario, the parameters of BP&DRC and BP&DDE should be carefully tuned to obtain the best visualization performance. On the contrary, the parameters setting of proposed method is robust and suitable for the different typologies of scenarios and several operating conditions. In fact, for the entire data set, the HMCA can assure good performance.

2.2.3 Computational cost of the algorithms

The average computational cost of the algorithms used in the evaluations are given in Tab.3. All reported results have been obtained using MATLAB version R2014a on an Intel Core i7 with CPU of 2.8 GHz on Microsoft Win7 operating system. AGC is the fastest algorithm among the methods. HMCA is almost as same as HE, PE in terms of operation speed while is faster than BD&DRC and BF&DDE.

Tab.3 Average computational cost of the algorithms in seconds

Image	AGC	HE	PE	BF&DRC	BF&DDE	HMCA
IM#1	0.014 1	0.020 6	0.023 9	2.711 3	2.586 5	0.024 6
IM#2	0.013 2	0.015 5	0.030 9	2.848 2	2.564 4	0.020 7
IM#3	0.016 9	0.016 4	0.018 7	2.570 8	2.624 6	0.022 0

3 Conclusion

In this paper, we have presented a new technique for dynamic range compression and detail

enhancement of IR images. The method consists of two steps. In the first step, dynamic range compression of infrared images is posed as an quadratic optimization problem that minimizes a cost function. In the second step, we enhance the local contrast using an exponential factor that provides an excellent visibility of details avoiding halo artifacts. We discussed thoroughly the choice of algorithm parameters and showed the effectiveness of the algorithm with real data. Subjective and quantitative performance comparisons are made for different IR image enhancement techniques. The results have shown that the proposed method can effectively reproduce the acquired signal in different scenarios, improve the overall contrast and enhance the target and image details. The proposed method has a very good application prospect such as night vision for driver assistance, surveillance in security, target signature measurement and tracking. It is worth noting that the proposed technique is a kind of nonlinear visualization methods, and the linear relationship between the digital level and the measured radiation is not maintained. Therefore it is not suitable for radiometric applications. Future developments on this subject are planned to implement the proposed algorithm in hardware.

References:

[1] Gonzalez R C, Woods R E. Digital Image Processing [M]. 2nd ed. Upper Saddle River: Prentice-Hall, 2002.

[2] Pizer S M, Amburn E P, Austin J D, et al. Adaptive histogram equalization and its variations[J]. *Computer Vision Graphics & Image Processing*, 1987, 39(3): 355–368.

[3] Chen H O, Kong N S P, Ibrahim H. Bi-histogram equalization with a plateau limit for digital image enhancement [J]. *IEEE Transactions on Consumer Electronics*, 2010, 55(4): 2072–2080.

[4] Liang K, Ma Y, Xie Y, et al. A new adaptive contrast enhancement algorithm for infrared images based on double plateaus histogram equalization [J]. *Infrared Physics & Technology*, 2012, 55(4): 309–315.

- [5] Arici T, Dikbas S, Altunbasak Y. A histogram modification framework and its application for image contrast enhancement [J]. *IEEE Transactions on Image Processing*, 2009, 18(9): 1921–1935.
- [6] Branchitta F, Porta A. Dynamic-range compression and contrast enhancement in infrared imaging systems[C]//SPIE, 2007, 6737(7): 076401.
- [7] Deng G. A Generalized unsharp masking algorithm[J]. *IEEE Transactions on Image Processing*, 2011, 20 (5): 1249 – 1261.
- [8] Polese A, Ramponi G, Mathews V J. Image enhancement via adaptive unsharp masking [J]. *IEEE Transactions on Image Processing*, 2000, 9(3): 505–510.
- [9] Branchitta F, Diani M, Romagnoli M. New technique for the visualization of high dynamic range infrared images [J]. *Optical Engineering*, 2009, 48(9): 096401.
- [10] Li M, Wei X, Zhao Y. Dynamic range compression and detail enhancement of infrared image [J]. *Journal of Computer-Aided Design & Computer Graphics*, 2014, 26 (9): 1460–1467.
- [11] Zuo C, Chen Q, Ren J. Display and detail enhancement for high-dynamic-range infrared images[J]. *Optical Engineering*, 2011, 50(12): 895–900.
- [12] Liu N, Zhao D. Detail enhancement for high-dynamic-range infrared images based on guided image filter [J]. *Infrared Physics & Technology*, 2014, 67: 138–147.
- [13] He K, Sun J, Tang X. Guided image filtering[C]//European Conference on Computer Vision, 2010: 1–14.
- [14] Monobe Y, Yamashita H, Kurosawa T, et al. Dynamic range compression preserving local image contrast for digital video camera [J]. *IEEE Transactions on Consumer Electronics*, 2005, 51(1): 1–10.
- [15] Peli E. Contrast in complex images [J]. *Journal of the Optical Society of America A – Optics Image Science and Vision*, 1990, 7(10): 2032–2040.
- [16] Celik T, Tjahjadi T. Contextual and variational contrast enhancement [J]. *IEEE Transactions on Image Processing*, 2011, 20(12): 3431–3441.